Exploring the morphology of mitochondria in breast cancer cells through fractal analysis in fluorescence imaging

Ferdania, Devi Fitri; Dhillon, Kiran; Kombrink, Sabrina; Samuel, Tony; Spill, Fabian

[Link to publication on Research at Birmingham portal](#)

Exploring the Morphology of Mitochondria in Breast Cancer Cells through Fractal Analysis in Fluorescence Imaging

Devi Fitri Ferdania, Kiran Dhillon, Sabrina Kombrink, Anthony Samuel, Fabian Spill

School of Mathematics, University of Birmingham

Introduction

A fractal object shows structure on all scales and often is self-similar. By self-similar, it means patterns at smaller scales resemble those at larger scales. To analyse such features, fractal geometry can be used as a mathematical and computational method to quantify and analyze the complex and self-similar patterns in the object. It operates on the principle that many natural and synthetic textures exhibit self-similarity across different scales. Two pivotal measurements in fractal geometry, fractal dimension and lacunarity, play crucial roles in assessing the complexity and irregularity of structures and quantifying the distribution of gaps within the objects, respectively.

Fractal patterns can be found throughout nature. For instance in the cellular system in our body, specifically mitochondria. Mitochondria are cell organelles that generate most of the chemical energy (adenosine triphosphate) needed to power the cell's biochemical reactions. Mitochondria also play roles in regulating cell metabolism, calcium signalling, and apoptosis (programmed cell death). However, in cancer cells, mitochondria become dysfunctional such as altered metabolism, mitochondrial DNA mutations, resistance to apoptosis, and altered morphology and dynamics. In this research, we mainly focus observing the change of mitochondrial morphology and dynamics which are controlled by a balance between mitochondrial fusion and fission events.

By integrating experimental data with mathematical modelling, we aim to discover and understand how changes in mitochondrial morphology and networking may contribute to chemoresistance. This approach seeks to predict patterns in mitochondrial behaviour in hypoxia, shedding light on potential mechanisms underlying cancer metabolism and drug resistance. Breast cancer cells were treated with Paclitaxel, a commonly used chemotherapy which stabilises microtubules to stop cancer cell proliferation. To study the effect of hypoxia and upregulation of HIF-1alpha (present in stiff breast tumours), mimicked hypoxia with Cobalt Chloride was used, and cells were treated with small molecule inhibitors of fission/fusion proteins DRP1/OPA1 to influence mitochondrial networks. Combinations of these conditions were investigated using live, time-lapse high resolution imaging of mitochondria.

Methods

A particular type of fractal dimension is box-counting dimension and is defined as follows

$$\dim_B(F) = \lim_{\epsilon \to 0} \frac{\log(N_\epsilon)}{\log(1/\epsilon)}.$$

where N_ϵ is the number of covers size ϵ to cover the object F. Figure 1 illustrates the box-counting algorithm. By observing how the count of boxes changes with the size of the boxes, information about the structure and complexity of the object can be obtained, and is encoded in the box-counting dimension.
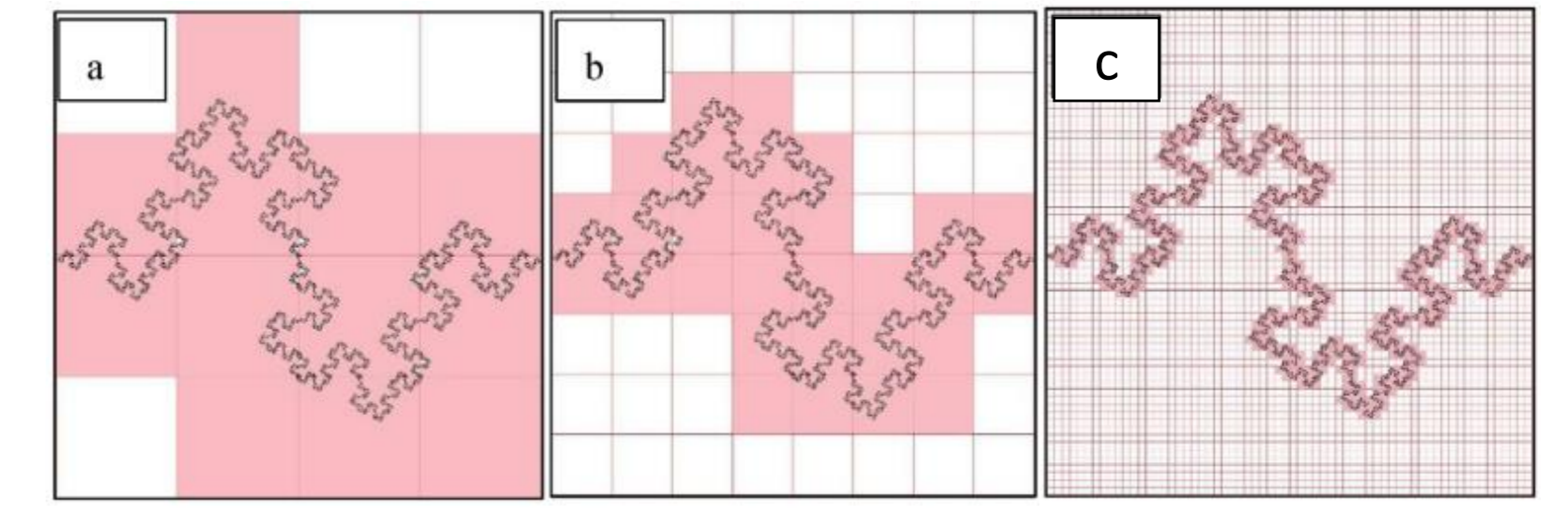

Figure 1. Box-counting method to approximate the box-counting dimension.

Lacunarity is calculated using FracLac, an ImageJ plugin. It calculates the lacunarity by first measuring the local heterogeneity for each box size ϵ as

$$\lambda_\epsilon = \left(\frac{\sigma_\epsilon}{\mu_\epsilon}\right)^2,$$

where σ_ϵ is standard deviation and μ_ϵ is the mean for pixels per box. Lacunarity is then calculated by the following formula

$$\lambda = \sqrt{\frac{\Sigma(\log(\lambda_\epsilon) - \mu)^2}{n}}.$$

Regarding the data, HCC106 Triple negative Breast cancer cells were cultured in RPMI + 5% FBS + 1% Pen/strep. Cells were treated with Cobalt Chloride 24 hours prior to imaging and further experimental conditions. For live, time-lapse imaging of mitochondria, cells were labelled with MitoTracker, DeepRed, and subsequently treated with various conditions of interests in complete culture medium with phenol-red free RPMI, 3 hours prior to imaging. Cells were imaged every hour for 21 hours, at 50X using CellDiscoverer7 (Zeiss).

We analysed seven groups of different treatment. Figure 2a shows the raw image from the microscope. The images were then processed by some image processing techniques, such as thresholding the intensity and adjusting the brightness and contrast. To segment the image, we used MitoMeter App, a MATLAB plugin. The example of a segmented image is shown in Figure 2b where the colour marks each mitochondrion object. Next, we cropped single cells from the last timestep in each treatment groups and convert them into binary images. Figure 2c displays a single cell sample from each treatment groups.
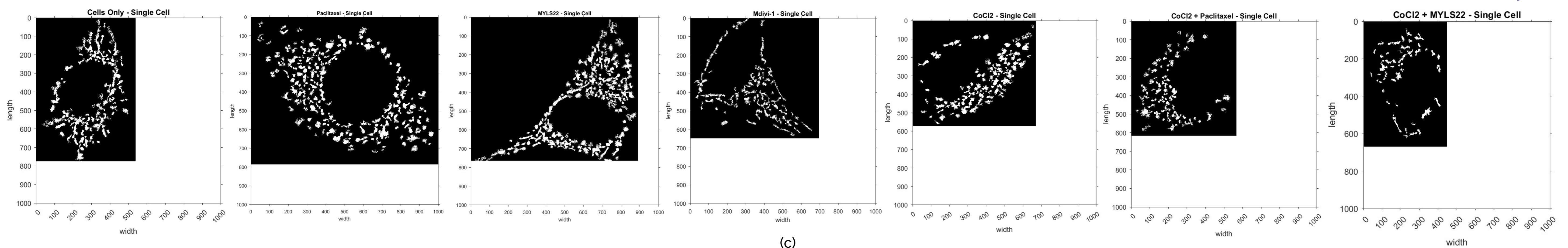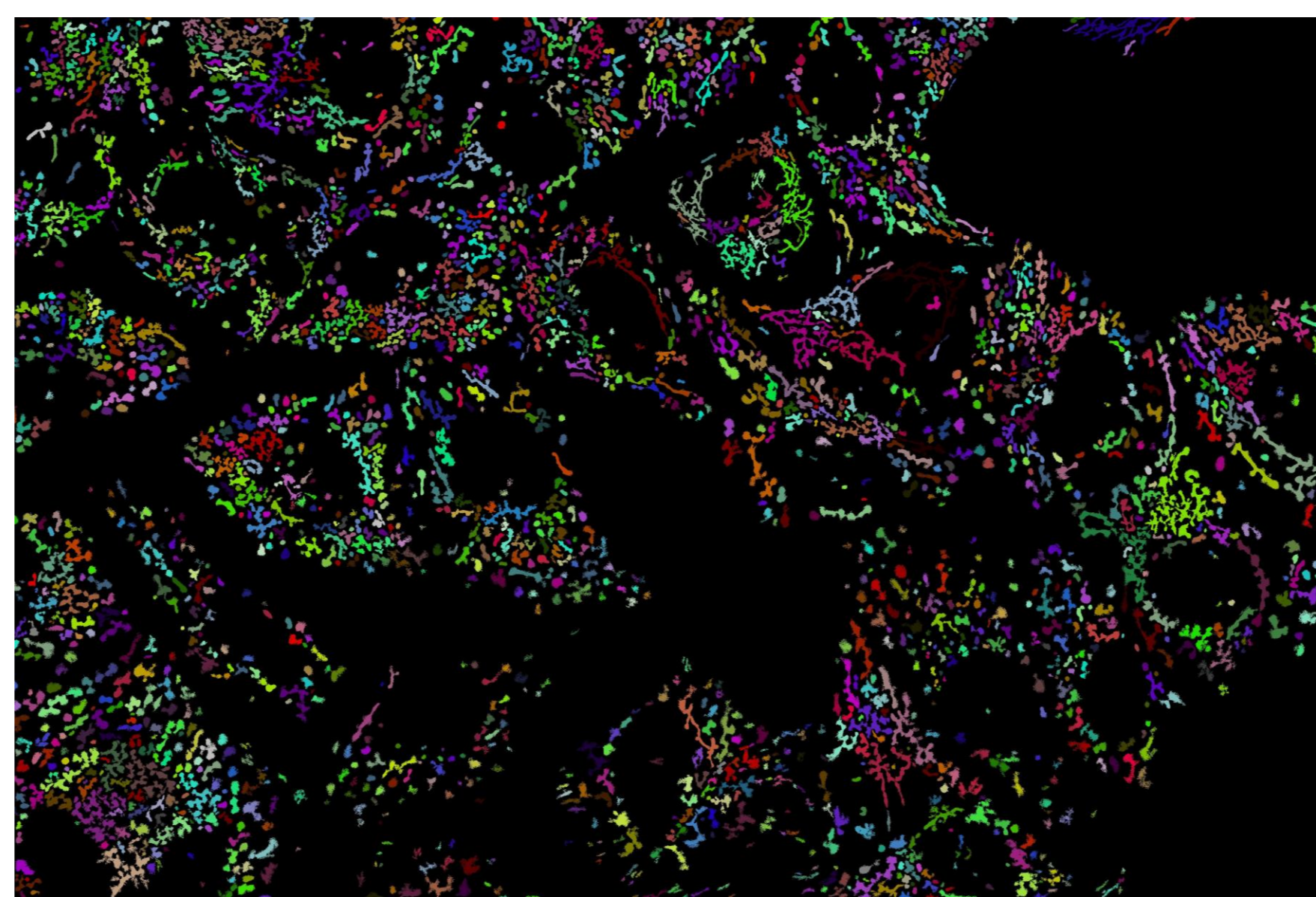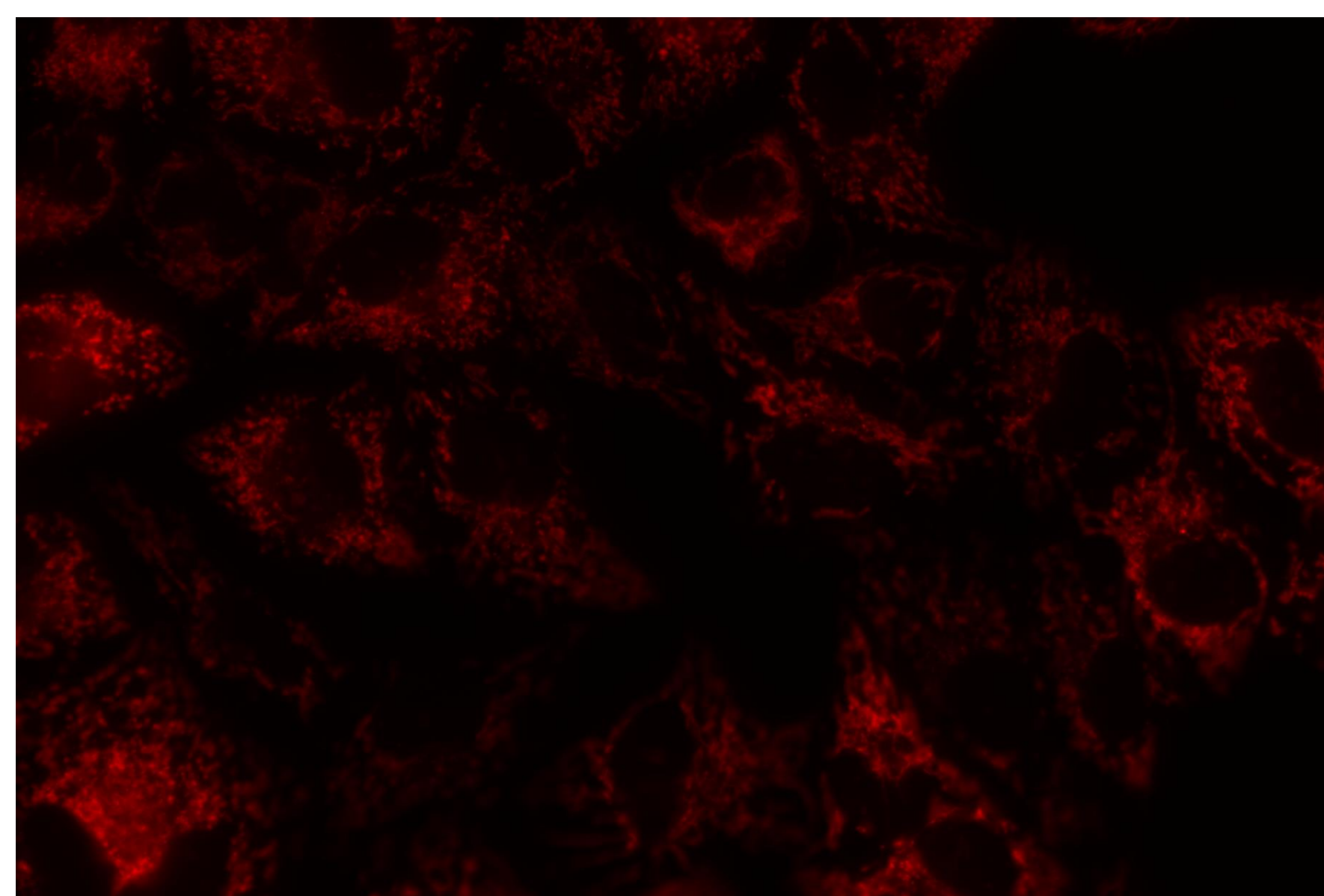

(a)

(b)

(c)

Figure 2. (a) Raw mitochondria fluorescence image from microscope, (b) the after processed and segmented image, and (c) single cell samples from (left to right) cells only group, Paclitaxel group, MYLS22 group, Mdivi-1 group, CoCl₂ group, combination of CoCl₂ and Paclitaxel group, and combination of CoCl₂ and MYLS22 group.
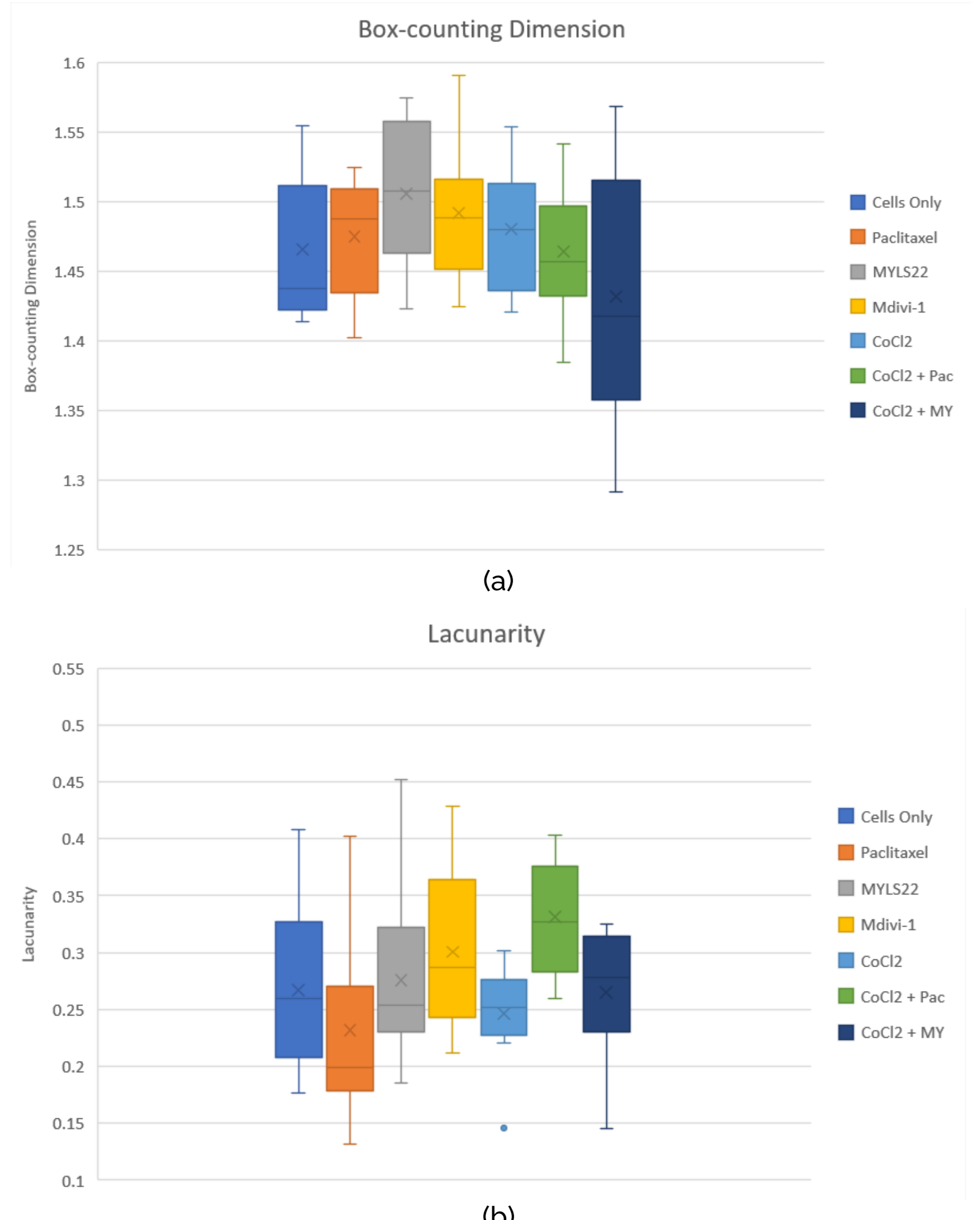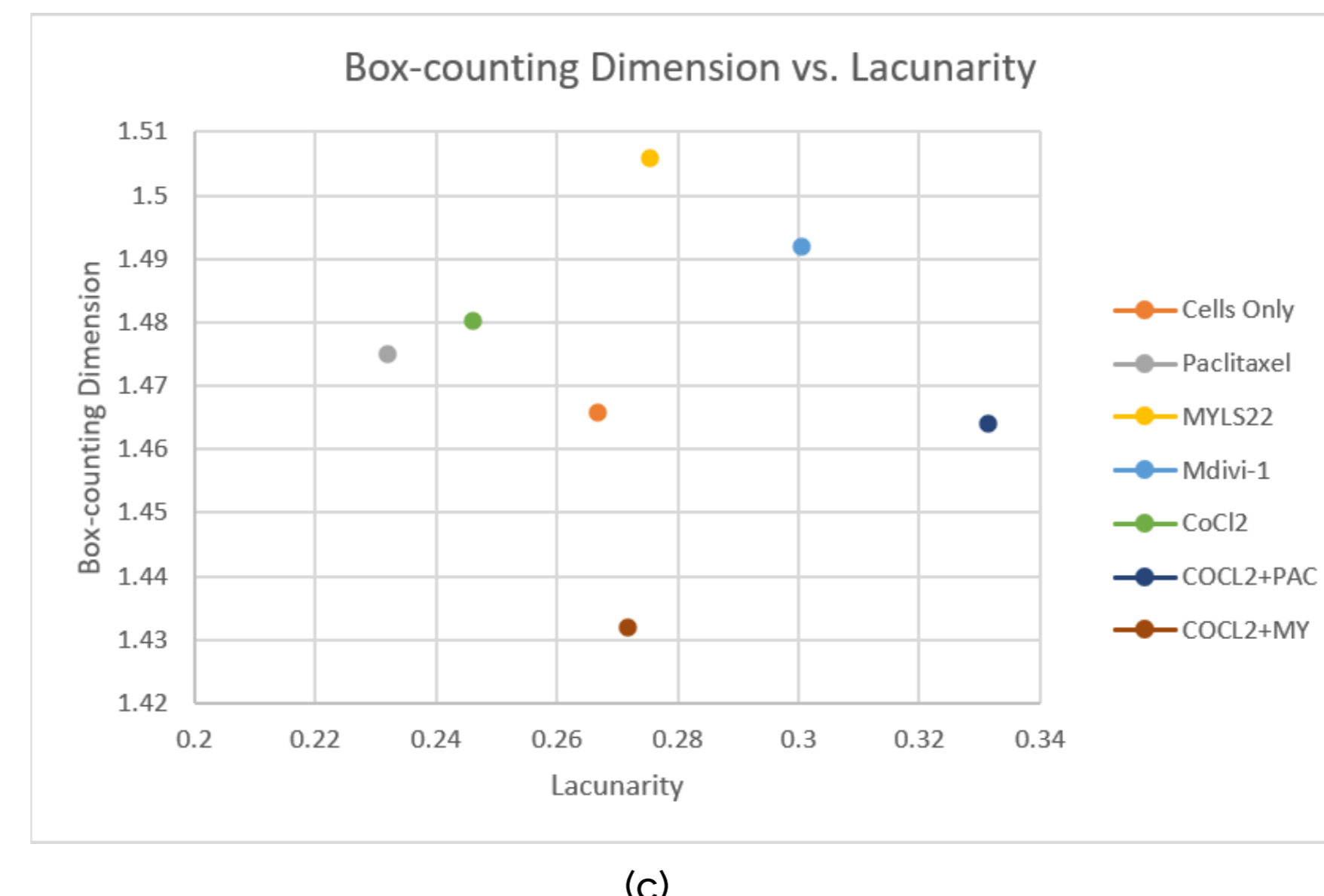
Results

(a)

(b)

Figure 3. (a) Box-counting dimension and (b) lacunarity box-plots for the single cells data. (c) Box-counting vs. lacunarity scatter plot based on the mean value for each treatment group.

A minimum of 20 single cells were analysed from each treatment group. Figure 3a illustrates that the CoCl2 + MYLS22 group exhibits the most significant variation in the box-counting dimension, while the MYLS22 group has the highest among all treatments. Figure 3b shows Paclitaxel group has the lowest lacunarity compared to other treatments. To make the analysis clearer, we plotted the mean values (lacunarity vs box-counting dimension) for each treatment group in Figure 3c. The control group, which is the Cells Only group, is in the middle of others as the image shows some mitochondria are elongated and some are in normal size. Also, they are all distributed equally around the nucleus and in the cytoplasm. Paclitaxel group has the lowest lacunarity as the mitochondria are completely segmented and distributed circular, very dense around the nucleus. Box-counting dimension and lacunarity of CoCl2 are slightly higher than Paclitaxel group as the mitochondria are also segmented but not as dense as the previous group.

(c)

Another group that has similar box-counting dimension is CoCl2 + Paclitaxel treatment. The cell samples of this group show that most of the mitochondria are segmented and dense in the half-side of nucleus only. It has the highest lacunarity among all the groups as the gap between mitochondria on the other side of the nucleus are larger. The CoCl2 + MYLS22 has the smallest box-counting dimension, but a middle value lacunarity. This happens because of the variations in the complexity of the sample cells. Some images show a big gap between mitochondria, but others are quite dense. Meanwhile, the last two groups (MYLS22 and Mdivi-1) depict the highest dimension compared to others. This is due to the branching-like structure which appears in the samples. In terms of lacunarity, Mdivi-1 is higher than MYLS22 group as most of the mitochondria are elongated leaving a bigger gap compared to the mostly fragmented mitochondria in the MYLS22. These phenomena match to the fact that MYLS22 inhibits the mitochondria to elongate and Mdivi-1 inhibits the mitochondria to divide.

Conclusion

We developed a method using invariants from fractal geometry to analyse how mitochondrial morphology and dynamics in breast cancer cells change when different treatments are given. Box-counting dimension and lacunarity were successful in differentiating and classifying various mitochondrial morphologies that happened in the samples. Box-counting dimension allows us to quantify the complexity of the mitochondria, while lacunarity inspects the porosity between each mitochondrion. In future work, we intend to analyse the images from the first time-step to the last and see how the box-counting dimension and lacunarity change over time. Some statistical tests and the increase in the number of samples will also be considered to get a more concrete conclusion.

References

- Chu, C.-H., Tseng, W.-W., Hsu, C.-M., & Wei, A.-C. (2022). Image Analysis of the Mitochondrial Network Morphology With Applications in Cancer Research. *Frontiers in Physics*, 10.
- Falconer, K. (2003). *Fractal Geometry* (pp. 27–38). John Wiley & Sons, Ltd.
- Lennon, F. E., Cianci, G. C., Kanteti, R., Riehm, J. J., Arif, Q., Poroyko, V. A., Lupovitch, E., Vigneswaran, W., Husain, A., Chen, P., Liao, J. K., Sattler, M., Kindler, H. L., & Salgia, R. (2016). Unique fractal evaluation and therapeutic implications of mitochondrial morphology in malignant mesothelioma. *Scientific Reports*, 6(1), Article 1.